CRYSTALLOGRAPHIC STUDIES USING QUADRUPOLE RESONANCE

Thesis for the Degree of M. S.
MICHIGAN STATE UNIVERSITY
Kenneth S. Robinson
1963

ABSTRACT

CRYSTALLOGRAPHIC STUDIES USING
QUADRUPOLE RESONANCE

By Kenneth S. Robinson

The interaction of the electric quadrupole moment of a nucleus (if the particular nucleus possesses such a moment) with the electric field due to surrounding charges in the crystal lattice gives rise to discrete energy levels, transitions between which energy levels can be induced by subjecting a specimen of the crystalline material to an oscillating magnetic field at a resonant frequency. This was accomplished by a super-regenerative radio frequency oscillator. If at the same time the crystal is subjected to a constant magnetic field of low intensity (Zeeman field) the degeneracy of the energy levels described above is removed and the spectral lines as viewed on the screen of an oscilloscope are split.

The separation of the components is a function of both the intensity of the Zeeman field and of the angle between the Zeeman field and the electric field gradient at the nucleus, being zero for certain values of the angle. If a stereographic plot is made of the direction of the Zeeman field at zero splitting of the spectral line, for various orientations of the crystal in the radio frequency

coil, the direction of the electric field at the nucleus can be determined. In this manner the number and orientations of inequivalent molecules in the crystalline unit call can be determined.

Studies were made of the splitting data for specimens of sodium chlorate, paradichlorobenzene, and cuprite. Both high and low temperature phases of paradichloro-benzene were observed.

CRYSTALLOGRAPHIC STUDIES USING QUADRUPOLE RESONANCE

By

Kenneth S. Robinson

A THESIS

Submitted to
Michigan State University
in partial fulfillment of the requirements
for the degree of

MASTER OF SCIENCE

Department of Physics and Astronomy

1963

DEDICATION

This thesis is dedicated to my wife, Ruth, for her love and patience during this period of study and research.

TABLE OF CONTENTS

LIST OF FIGURES

CHAPTER I

THEORY

The potential of a distribution of charged nuclear matter may be expressed in the series,

$$\phi(r,\theta) = \frac{e}{r}\left[Z + \frac{P}{r}\cos\theta + 1/2\,\frac{Q}{r^2}(3\cos^2\theta - 1) + \ldots\right]^{1} \quad (1)$$

In the first term ze represents the monopole charge distribution and determines the coulomb potential of the nucleus. P represents the electric dipole moment of the nucleus. It can be shown, from parity considerations, backed by experimental evidence,[1] that the electric dipole moment of any nucleus is zero. The quantity Q specifies the electric quadrupole moment of the average nuclear charge distribution. This quantity is zero for spherically symmetric charge distributions, as well as for nuclei of spins zero and one-half. Charge distributions represented by a prolate ellipsoid possess positive nuclear electric quadrupole moments, and a negative Q corresponds to an oblate ellipsoid distribution. For example, the electric quadrupole moment of the deuteron has a value of $+ 2.73 \times 10^{-27}$ cm^2, showing that the ground state of this nucleus is not a pure s state of zero orbital angular momentum.

A strong coupling between the electric quadrupole moment of a nucleus and the electric field gradient at the nucleus due to surrounding charges produces quantized energy levels between which transitions may be observed under proper circumstances. This phenomenon is known as pure nuclear quadrupole resonance.

It should be emphasized that these energy levels are caused by a coupling of two electric systems present within the atom, in contrast to nuclear magnetic resonance, which results from the application of a strong external magnetic field, which then interacts with magnetic dipole moment of the nucleus.

To observe the quadrupole resonance spectra, transitions between the energy levels must be brought about by absorption of energy supplied from some external source, and for maximum probability of such transitions, energy must be supplied at a frequency such that the condition, $h\nu = E_{m+1} - E_m$ is satisfied. In principle, several mechanisms for supplying such energy to the nucleus present themselves, but practical considerations eliminate all but one. Since nuclei do not possess electric dipole moments, the only way an oscillating electric field could be used is to couple it with the quadrupole electric moment of the nucleus. However, to induce a sufficient number of transitions by this method, electric field gradients too large to generate in the laboratory would be required. In practice,

an oscillating magnetic field is coupled with the magnetic dipole moment of the nucleus, to "shake" the nucleus and cause transitions between energy levels resulting from coupling of the electric quadrupole moment of the nucleus and the field gradient at the nucleus due to surrounding charges. It is evident that definite energy levels will exist only if the average field gradient at the nucleus is constant in time, hence nuclear quadrupole resonance is observed only in crystalline solids.(2)

If the electric field at the nucleus has cylindrical symmetry, quantum-mechanical theory gives the following expression for the above energy levels--(3)

$$E_m = \frac{e^2 q Q}{4I(2I-1)} \left[3m^2 - I(I+1)\right] \qquad (3)$$

where I represents the nuclear spin number, m the magnetic quantum number. The expression e^2qQ is called the quadrupole coupling constant, where $eq \equiv V_{zz}$ is the component of the field gradient tensor in the direction of the symmetry axis and eQ represents the electric quadrupole moment of the nucleus.

For equation (3), it can be seen that the states ψ_{+m} and ψ_{-m} possess equal energies, since only even powers of m appear, and that therefore for nuclei of half-integral spin there are I + 1/2 doubly degenerate energy levels, since m may take on values I, I - 1, 1 - 2,. . . -I.

If now a weak constant magnetic field H_o, (Zeeman field) is applied at an angle θ, this degeneracy is removed and for a given $|m| > 1/2$, there are two energy levels--(3)

$$E_{\pm} = \frac{e^2qQ}{4I(2I-1)} \left[3m^2 - I(I+1) \right] \mp m \hbar \Omega \cos \theta \qquad (4)$$

where $\Omega = \gamma H$ represents the angular frequency of the Larmor precession of the nucleus in the magnetic field. For $|m| = 1/2$, a special quantum mechanical case arises, in which mixing of the $\psi_{+1/2}$ and $\psi_{-1/2}$ states forms new states, $\psi_{\pm}$, having energies given by --(3)

$$E_{\pm} = A \left[3/4 - I(I+1) \mp \frac{f}{2} \hbar \Omega \cos \theta \right] \qquad (5)$$

where $A = \frac{e^2qQ}{4I(2I-1)}$ and

$f = \left[1 + (I + 1/2)^2 \tan^2 \theta \right]^{1/2}$.

Since (4) represents energy states for $|m| > 1/2$, and (5) represents energy states for $|m| = 1/2$, transitions can occur between two energy levels, one being either one of the levels (4) and the other being either one of the levels (5). For the case $I = 3/2$ the resulting four transitions are shown in the accompanying diagram.

The lengths on the diagram, labeled $\alpha, \alpha', \beta, \beta'$ bear no relationship to the intensities of the spectral lines resulting from these transitions.

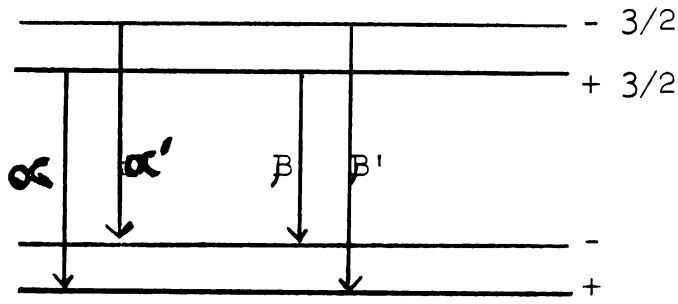

Fig. 1.--Energy level transitions for nuclei of spin 3/2, after removal of degeneracy by application of Zeeman field.

If each of the energies in (4) is, in turn, subtracted from each of the energies in (5) and if the resulting expression is divided by $\hbar$, to give angular frequency ω, the following frequencies[3] are obtained--

$$\omega_\alpha = \frac{6A}{\hbar} - \frac{3-f}{2}\Omega\cos\theta$$

$$\omega_\beta = \frac{6A}{\hbar} - \frac{3+f}{2}\Omega\cos\theta$$

$$\omega_{\alpha'} = \frac{6A}{\hbar} + \frac{3-f}{2}\Omega\cos\theta$$

$$\omega_{\beta'} = \frac{6A}{\hbar} \quad \frac{3+f}{2}\Omega\cos\theta$$

Here f represents the absolute value of the radical, and the α and β components differ only in the sign assigned to f. In this sense there is no real physical difference between the α and β, and the α' and β' components.

The splitting of the α components is expressed by

$$\omega_{\alpha'} - \omega_\alpha = (3-f)\Omega\cos\theta$$

Setting this quantity equal to zero, and assuming cos $\theta \neq 0$ we get $f = [1 + (I + 1/2)^2 \tan^2 \theta]^{1/2} = 3$,

$$\tan^2 \theta = \frac{8}{(I + 1/2)^2} \quad \text{and}$$

$$\theta = \arctan \frac{2\sqrt{2}}{I + 1/2} \quad \arctan \sqrt{2} \quad \text{for } I = 3/2 . \quad (8)$$

Cos θ can be assumed unequal to zero, for zero splitting, since for $\theta = 90°$ the splitting is $(I + 1/2)\Omega$, as can be seen by substituting the expression for f in (7), and simplifying.

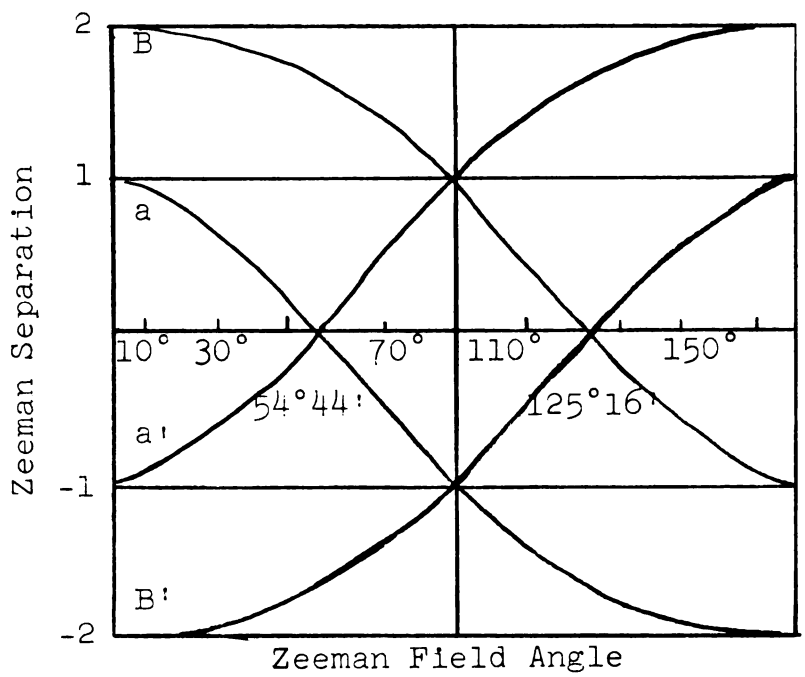

Fig. 2.--Theoretical plot of separations of resonance line components as a function of orientation of the Zeeman field. Separations are in units of $\Omega = \gamma H$.

The splitting of the β component is expressed by $\omega_{\beta'} - \omega_{\beta} = (3 + f)\Omega \cos\theta$. This expression vanishes for $f = -3$, which occurs for $\theta = 125°16'$. In summary of the above discussion, it is stated that, for the case $I = 3/2$ zero splitting of the α component of the quadrupole resonance line occurs when the angle between the Zeeman field and the field gradient at the nucleus is approximately $54°44'$, and zero splitting of the β component occurs at $\theta = 125°16'$.

Quantum-mechanical theory gives the ratio of the intensities of the β component to the α component as f-1 / f+1, so that the α pair is always more intense than the β pair. Note that here f is an absolute value. For zero splitting of the α line, this ratio becomes 1/2, making the zero splitting condition relatively easy to determine experimentally, since generally there will be a strong line formed by the coalescing of the α components.

It can be seen that, for zero splitting, the direction of the Zeeman field is an element of a right circular cone of semivertical angle $54°44'$ (for $I = 3/2$). The axis of the cone of zero splitting is a symmetry axis of the electric field gradient at the nucleus. Hence the directions of the symmetry axes of the electric fields in the specimen can be determined experimentally, and if the symmetry axis of the crystal is known by other means, such as crystallographic measurements, then the orientations of the electric field gradients within the unit cell of the crystal can be determined.

The Hamiltonian for the interaction of the electric quadrupole moment of the nucleus with the electric field at the nucleus due to the surrounding charges in the crystal lattice can be expressed as

$$H_Q = \frac{eQ}{4I(2I-1)} \left[V_{zz} \left(3I_z^2 - I^2\right) + \left(V_{xx} - V_{yy}\right) \left(I_x^2 - I_y^2\right)\right]$$

It can be seen from the above that only two parameters are needed to characterize the derivatives of the potential--V_{zz} and $V_{xx} - V_{yy}$. The asymmetry parameter,

$$\eta = \frac{V_{zz}}{V_{xx} - V_{zz}} \quad , \text{ or what is equivalent,}$$

$$\eta = \frac{\frac{\partial E_x}{\partial X} - \frac{\partial E_y}{\partial Y}}{\frac{\partial E_z}{\partial Z}}$$

is defined to express the departure of the charge configuration of the nucleus from cylindrical symmetry. A nucleus may originally possess a symmetrical field but this symmetry may be destroyed by intermolecular forces in the crystal lattice. Thus in the free tetrahalide molecule there is three-fold symmetry about each halogen bond, but in the crystalline state intermolecular forces destroy this symmetry.

In all the previous discussion it was assumed that an axially (or cylindrically) symmetric electric field existed at the nucleus (asymmetry parameter = 0). In many cases, including those studied here, η is small enough that it can be disregarded. In fact, one piece of information obtained from nuclear quadrupole resonance measurements is an upper limit to the value of the asymmetry parameter.

CHAPTER II

EXPERIMENTAL TECHNIQUES

Since the electric field gradient at the nucleus is principally due to the valence electrons of the atom, determination of this gradient can provide useful information about the binding of the atom in the crystal. While in principle the gradient can be determined by measurements of the intensity ratio of the α and β components, f - 1/f + 1, it is more feasible experimentally to measure the dependence of the splitting of the α component on the direction of the magnetic field. This requires the following apparatus:

1. A means of subjecting the sample to a radio frequency magnetic field whose frequency can be swept through the desired region.
2. A means of detecting the resonant energy absorption.
3. A method of applying a constant magnetic field in the Zeeman region to the specimen.
4. A method of analyzing, visualizing, and unraveling the loci of zero splitting for each of the symmetry axes of the unit cell.

With respect to one and two above, considerably more radio frequency power is required than in nuclear magnetic resonance experiments, because of the smaller lattice

relaxation times. The sensitivity of the detection apparatus must be sufficient to give a measureable signal above the noise level of the oscillator and amplifier. In nuclear magnetic resonance it is possible to hold the radio frequency field at a constant frequency and search for resonance by varying the Larmor frequency of the nucleus by means of slowly varying magnetic field. In quadrupole resonance, the nuclear frequencies are fixed by the crystalline structure and provision must be made for sweeping the applied radio frequency back and forth over the resonant frequency of the nucleus. If this is done at a constant rate, absorption will occur each time the resonant frequency is passed through.

The above requirements are fulfilled by the self-quenching super-regenerative oscillating detector, a form of which is shown in the accompanying diagram. The sample is placed in a radio frequency coil, L_1 and the voltage level of oscillation becomes a function of energy absorption from the tuned circuit by the nuclear spin system. The oscillations in the tank circuit are quenched by the charging of the capacitor C_4, the rate of quenching being determined by the R_1C_4 time constant. This causes the specimen to be subjected to bursts of radio frequency energy. If energy is absorbed from the circuit by the specimen, the discharge of C_2 will be hastened and the radio frequency bursts will be initiated earlier by nuclear

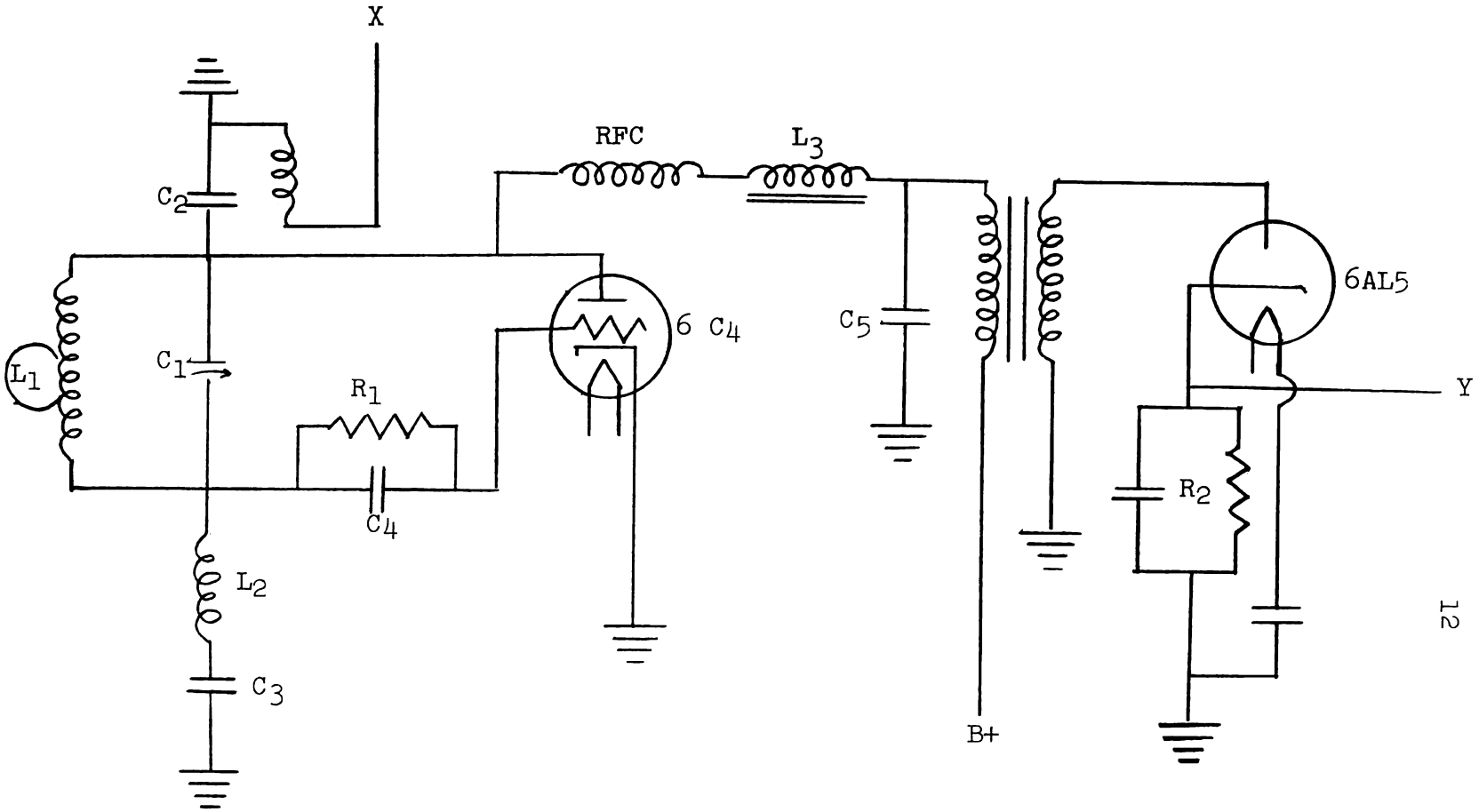

Figure 3. Superregenerative Detector Used to Supply Radio Frequency Energy to Crystal.

L_1 = Radio Frequency Coil

L_2,C_3 = Regeneration Control

L_3 C_5 = Quench Frequency Filter

C_1 = Tuning Condenser

C_2 = Vibrating Condenser

R_1,C_4 = Quench Frequency Circuit

6AL5 = Detector

X = 60 Cycle Power to Vibrating Condenser

Y = To Oscilloscope

signal. This results in a still greater absorption of energy and provides the high signal to noise ratio inherent in this detector. The voltage appearing across R_2 is applied to the vertical deflection plates of a cathode ray oscilloscope, and if, periodically, energy is absorbed from the circuit, a signal is seen on the screen of the oscilloscope. In the arrangement used the quench frequency was found to be of the order of 50 kilocycles.

Provisions is made for sweeping back and forth over the quadrupole resonant frequency of the nucleus by the vibrating condenser, C_2 which is driven by the line voltage and which frequency modulates the oscillator. Thus 120 times per second energy is absorbed from the circuit by the spin system of the nucleus, provided the oscillator is tuned to the proper range.

A problem which arises in connection with the use of the self-quenched superregenerative detector is that of the side bands occuring at integral multiples of the quench frequency on either side of the fundamental frequency. Resonance can occur at any of these side band frequencies, if it possesses sufficient energy, as the oscillator is swept through its range, thus leading to confusion concerning the correct resonant frequency. This confusion can be overcome by varying the quench frequency and observing the resonant line which does not shift. The author has also found that one can vary

the oscillator frequency and count the resonances appearing, and choose the central one of these as the fundamental.

The Zeeman field of three above, is supplied by a double Helmholtz coil of radius about 11 cm. and having about 500 turns on each coil. This provides a uniform field at the center of about 36 gauss when one ampere of current exists in the coil. The coil is arranged so that it can be rotated about a vertical axis. Since the crystal is arranged in the cavity of the oscillator coil in such a way that it can be rotated about a horizontal axis, it becomes possible to sweep the magnetic field over the crystal from all directions. This obviates the inconvenience of actually orienting the magnetic field over the entire sphere.

The problem of four above is met in the following manner. The zero-splitting data will now consist of a set of ordered pairs of numbers, representing the angular settings of the crystal in its rotation about a horizontal axis, and of the Helmholtz coil about a vertical axis, respectively. This data can best be analyzed, and the zero-splitting can best be visualized, by plotting this data on a stereographic net, which, in effect, accomplishes stereographic projection.

In the stereographic projection, a point is projected from the surface of a sphere onto a plane which is perpendicular to an axis of the sphere and passes through

the center of the sphere, by passing a line from the point to the pole of the sphere which lies on the opposite side of the plane, the intersection of the line with the plane being the projection of the point. The distinguishing characteristic of the stereographic projection is that a small circle on the surface of the sphere projects as a circle (or the limiting case of a circle, a straight line).

In effect the cone of zero-splitting intersects the surface of the imaginary sphere in a circle, which is then projected onto the plane of the paper. It then becomes a simple matter to draw the best arcs through the projected points, or to fit a theoretical plot to the data, if the unit cell structure is known from other sources. The center of the projected circle is the symmetry axis of the electric field gradient present at the nucleus.

CHAPTER III

EXPERIMENTAL RESULTS

The structure of crystalline sodium chlorate is well known, as a result of x-ray diffraction work. Sodium chlorate has a cubic structure, with the unit cell containing four molecules, each molecule containing a Na^+ ion and a ClO_3^- ion. The ClO_3^- ions form a pyramid with the three oxygen atoms at the vertices of the base, the chlorine atom at the apex, and the lines connecting the chlorine and the sodium nuclei being parallel, respectively to each of the four body diagonals of the unit cell. Therefore a three-fold symmetry exists about each body diagonal. Since the Cl^{35} nucleus has spin 3/2, and since the electric field gradient is symmetric about the sodium chlorine axis, equation (7) gives 54° 44' for the value of the semivertical angle of the cone of zero-splitting about each field gradient. Figure 4 is a theoretical stereographic plot of the loci of zero-splitting for the chlorine nucleus in $NaClO_3$, when the crystal is rotated about a body diagonal. There are four physically inequivalent sites in the unit cell, for which the symmetry axes of the electric field gradients are represented by points labeled A, B, C, the fourth symmetry axis being

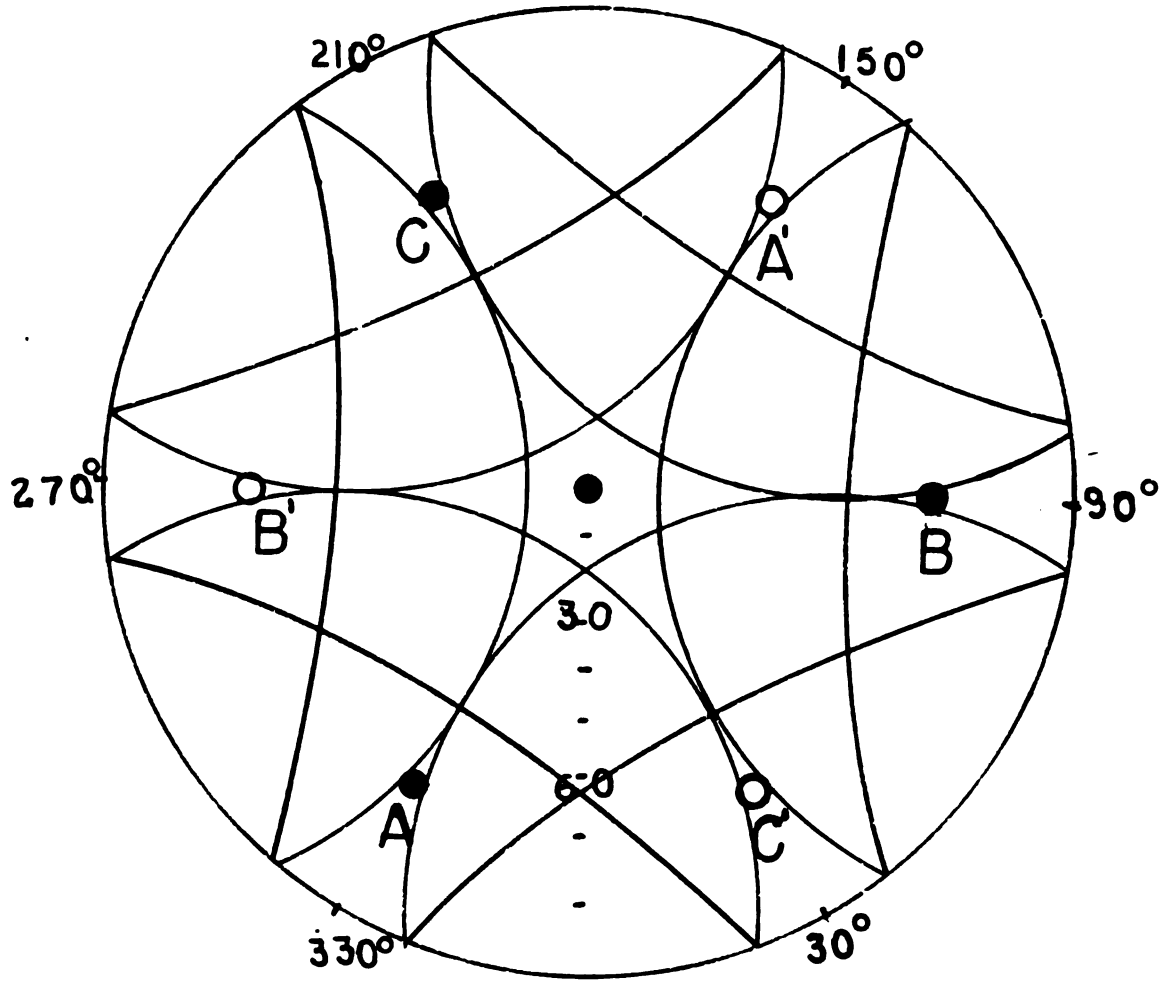

Fig. 4.--Theoretical Stereographic Plot of Zero-Splitting for Cl^{35} Nucleus in $NaClO_3$, Showing 3-fold Symmetry about a Body Diagonal.

represented by the dot at the center, coinciding with the north-south axis of the projecting sphere.

Points A, B, C, are separated from the center by 70° 32' on the stereographic net, which is the angle formed by the intersection of the body diagonals of a cube, and are separated from each other by 109° 28'. Since the cone of zero splitting has a semivertical angle of 54° 44', its intersection with the projecting sphere will be a circle, the major arc of which lies above the projection plane, or primitive circle, and the rest below. The smaller arc about each point represents a projection from below the plane.

Since the cone of zero-splitting has two surfaces, or nappes, there will be associated with each of the points A, B, C, a point A', B', C' representing the other end of the field gradient symmetry axis, surrounded by projected arcs representing the other nappe of the cone. In this case the larger arc is projected from below and the smaller from above. It should be pointed out that the points representing the field gradient axes are at the physical centers of the arcs, as measured on the stereographic net, and not at the geometric centers.

Figure (5) represents the zero-splitting data for sodium chlorate rotated about a 3-fold axis, with the theoretical plot of figure (3) superimposed. Regions of the curve which were deficient in data points were searched again

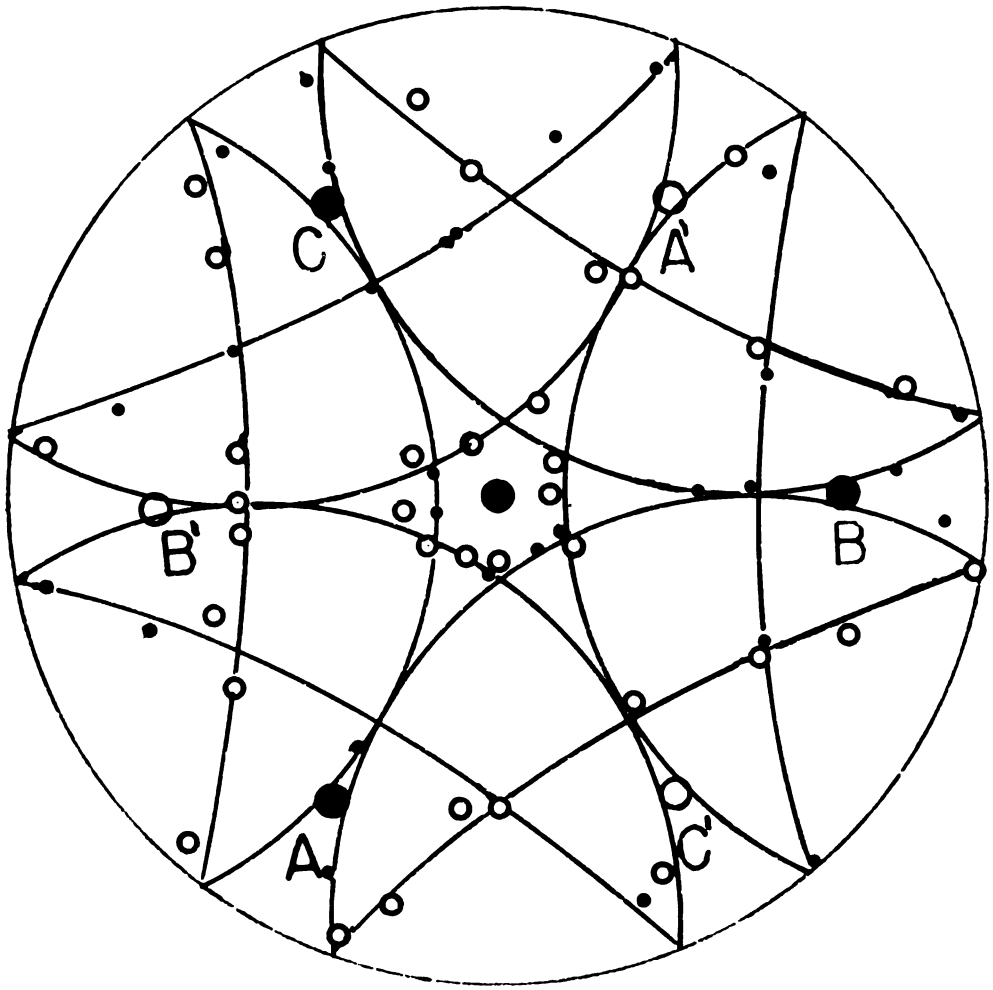

Fig. 5.--Zero-Splitting Data for NaClO, With Theoretical Plot for Fig. 3 Superimposed.

experimentally. In some cases broadening of the spectral line made it impossible to separate signal from noise in these regions. The departure of some of the experimental points from the expected curves is evidence, perhaps, of imperfections in the crystal lattice. In some of the specimens studied later this effect was quite pronounced. Solid dots represent points projected from the upper hemisphere onto the projecting plane, and open dots represent points projected from the lower hemisphere upward onto the plane.

Figure 6 is a stereographic projection of the zero-splitting data for a crystal of paradichlorobenzene $C_6H_4Cl_2$, which was freshly grown from the melt. The splitting was carried out at a temperature of about 25°C. Since this crystal was grown in a piece of glass tubing which had been pulled out to a fine tip and lowered slowly into cold water, there were no observable faces and no crystalline orientations were known. Therefore it was impossible to construct a theoretical plot of the splitting. However, the plot shows quite clearly that there was only one molecular orientation in sufficient abundance to produce strong signals. The presence of points some distance from the curves is evidence that phase transitions had taken place. In this specimen the field gradient axis AA' is inclined at an angle of about 72° 30' with the axis about which the crystal was rotated,

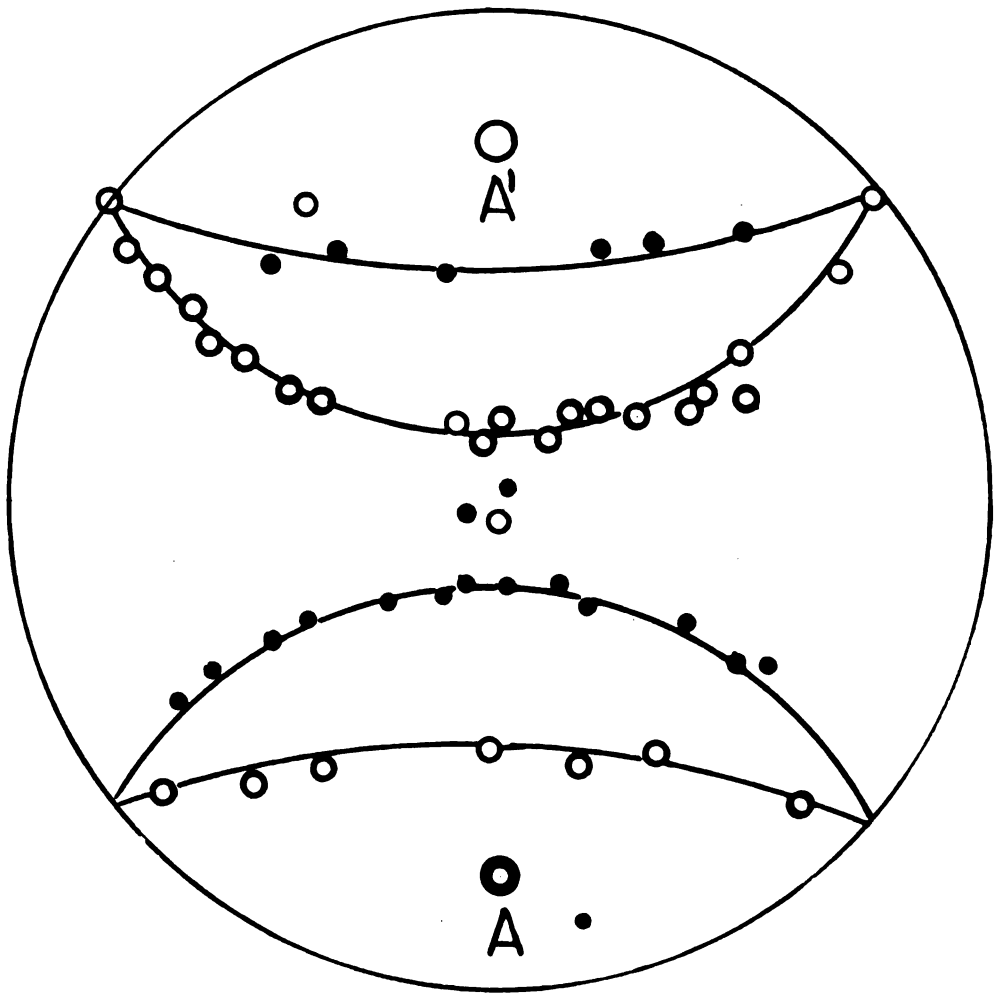

Fig. 6.-- Stereographic Projection of Zero-Splitting Data for Paradichlorobenzene Crystal, High Temperature Phase.

according to measurement on the stereographic net. This measurement was predicated on the assumption that, since Dean and Pound[4] had found the value of the asymmetry parameter for Cl_{35} in paradichlorobenzene to be 0.08I 0.03, then the predictions of theory as discussed previously here apply, within the limits of experimental methods used here, and so the zero-splitting angle is 54° 44'. This crystal evidently was in the high temperature (β) phase and this is consistent with the results reported by Dean and Pound[4], in which they report that the backward transition from β to α phase occurred slowly on cooling from the melt, and could not be accelerated by cooling below 22°C.

Figure 7 is for a crystal of paradichlorobenzene which had been grown from melt some years before. Here there are two molecular orientations, AA' and BB', making an angle between them, as measured from A to B on the stereographic net, of about 75°. This agrees with results given by Dean and Pound[4], which gives the angle between the Cl-Cl direction (Z axis) and the symmetry axis of the monoclinic crystal (b axis) the value 52° 30'. The two molecules in the unit cell are related by rotation through 180° about the b axis. By locating a point on the stereographic net at an angular distance of 52° 30' from both A and B' the b axis of the crystal was located

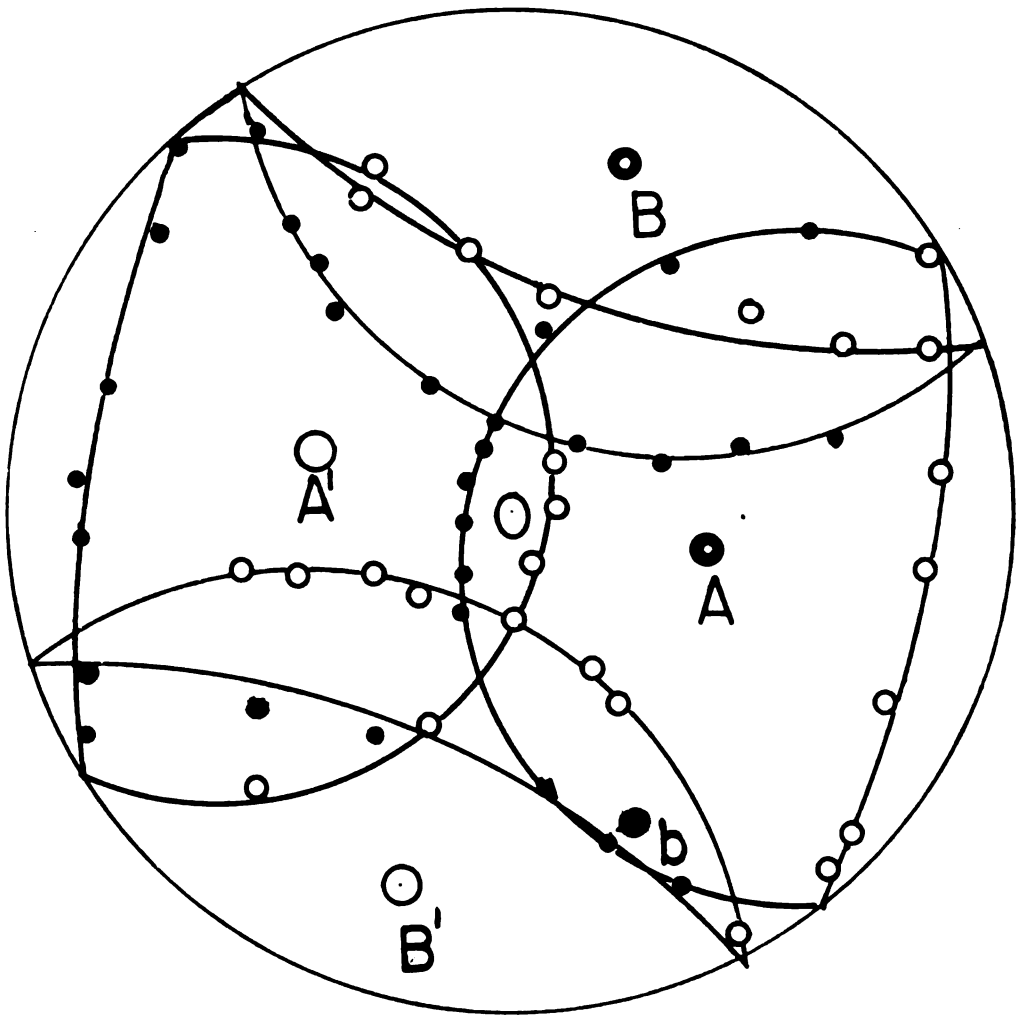

Fig. 7.--Stereographic Projection of Zero-Splitting Data for Paradichlorobenzene Crystal, Low Temperature Phase.

at the point marked 'b', at an angle of about 68° from the axis about which the crystal was rotated.

Resonant frequency in the α (low temperature) phase was measured at 34.16 megacycles, at about 25°C. Duchesne and Nonfils [5] have measured the resonant frequency at 34.28 megacycles at 21°C and Buyl-Bodin and Dantreppe [6] obtained a value of 34.16 mc.

It would be instructive to carry out splitting measurements on the specimen of figure 5 at intervals over a period of time, in an effort to observe the transformation from the β phase to the α phase.

Figure 8 is a theoretical plot of the splitting pattern of a single crystal of cuprite (Cu_2O), rotated about a line parallel to the edge of the unit cell. X-ray data [7] indicates that the unit cell of cuprite is cubic, containing two molecules, with each oxygen atom at the center of a regular tetrahedron having a copper atom lying midway between the two oxygen atoms. Since the oxygen-copper-oxygen axis is the symmetry axis of the electric field gradient present at the copper nucleus, there are four physically inequivalent copper sites, with the field gradients parrallel to the body diagonals of the cube.

Since the angle between a body diagonal and an edge of the cube is 54° 44', the same as the angle of zero-splitting all the cones of zero splitting pass through the

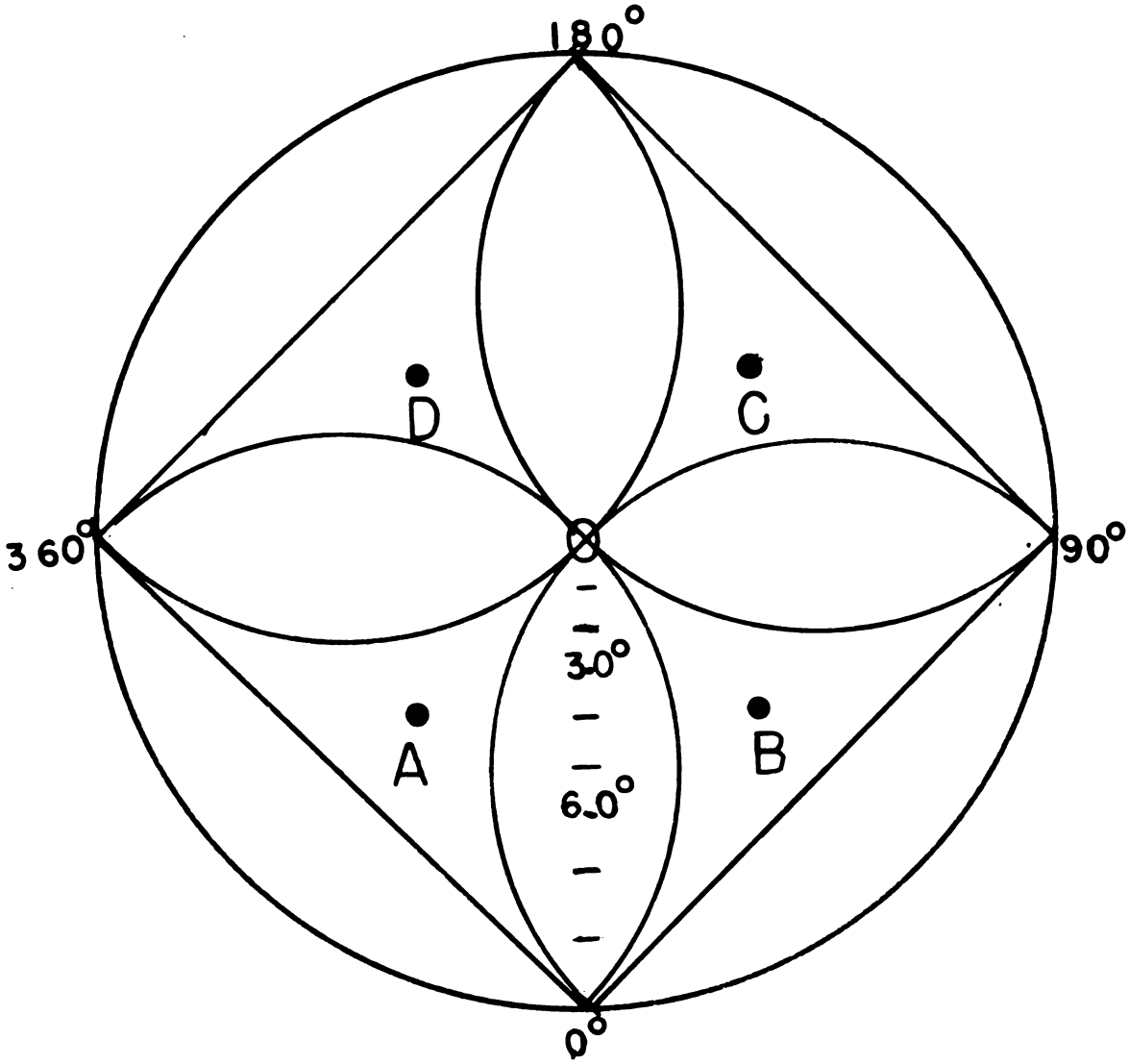

Fig. 8.--Theoretical Plot of Zero-Splitting of Cuprite Crystal, about Axis Parallel to Edge of Unit Cell.

center point of the diagram, the axis about which the crystal was rotated. In this case elementary spherical trigonometry shows that the smaller arc of the circle of intersection of the cone with the sphere projects onto the plane as a straight line. Also, the projection of the second nappe of the cone about A coincides with the projection of the first nappe about C, and likewise for each of the other cones.

Figure 9 represents the theoretical plot of figure (7) superimposed on the stereographic projection of the splitting data for a cuprite specimen. This specimen was cut from a matrix containing several octahedral cuprite crystals and was by no means a single crystal. In fact, one of the principal difficulties in nuclear quadrupole resonance work is that of obtaining single crystals of sufficient volume to provide a strong absorption signal. The specimen of figure 8 appears to consist of a single large crystal with parts of two or three other crystals adhering to it. Since the specimen did exhibit several well defined faces, it was possible, by goniometric measurements, to determine a probable symmetry axis about which to rotate it. The fit of figure 9 is evidence for the above statement.

The resonant frequency of the specimen was measured at 25.94 megacycles. Williams[8] gives the frequency at about 26 megacycles for Cu^{63} and about 24 megacycles for Cu^{65}.

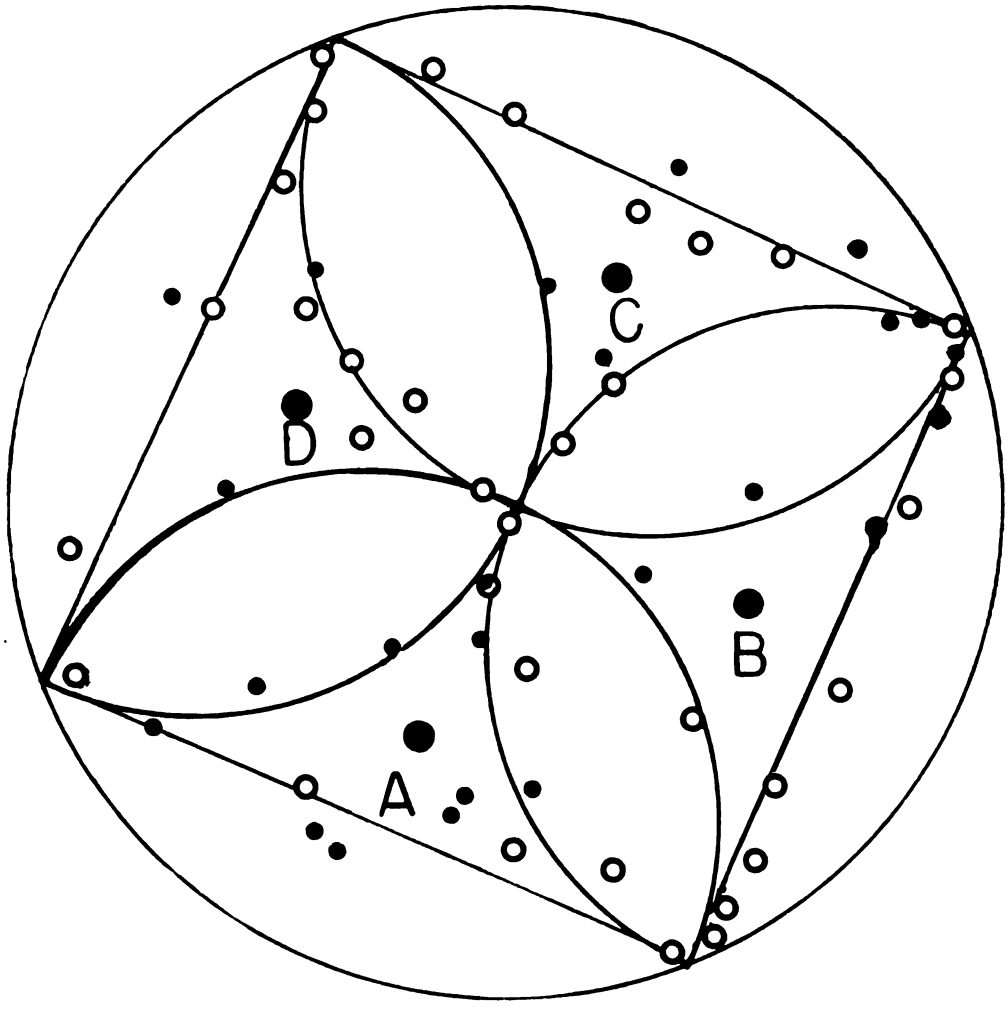

Fig. 9.--Splitting Data for Cuprite Crystal, with Theoretical Plot of Fig. 7 Superimposed.

It is evident that quadrupole resonance can be a very effective tool for dealing with problems of crystal structure. In particular, one can use it--

a. To locate crystallographic axes. This application is especially useful when the specimen exhibits no well-defined faces, so that goniometric measurements are not possible, as in the case of the paradichlorobenzene crystal which was studied.

b. To determine the number of nonequivalent molecules in the unit cell. Chemically nonequivalent molecular sites exhibit nultiple lines in the pure quadrupole spectrum while physically nonequivalent molecules can be distinguished by a study of zero-splitting data.

c. To determine the order of the crystallographic axes.

d. To study phase transitions. As indicated previously, day to day observation of the transition of paradichlorobenzene from the high temperature, β phase to the low temperature, α phase is an intriguing possibility.

APPENDIX

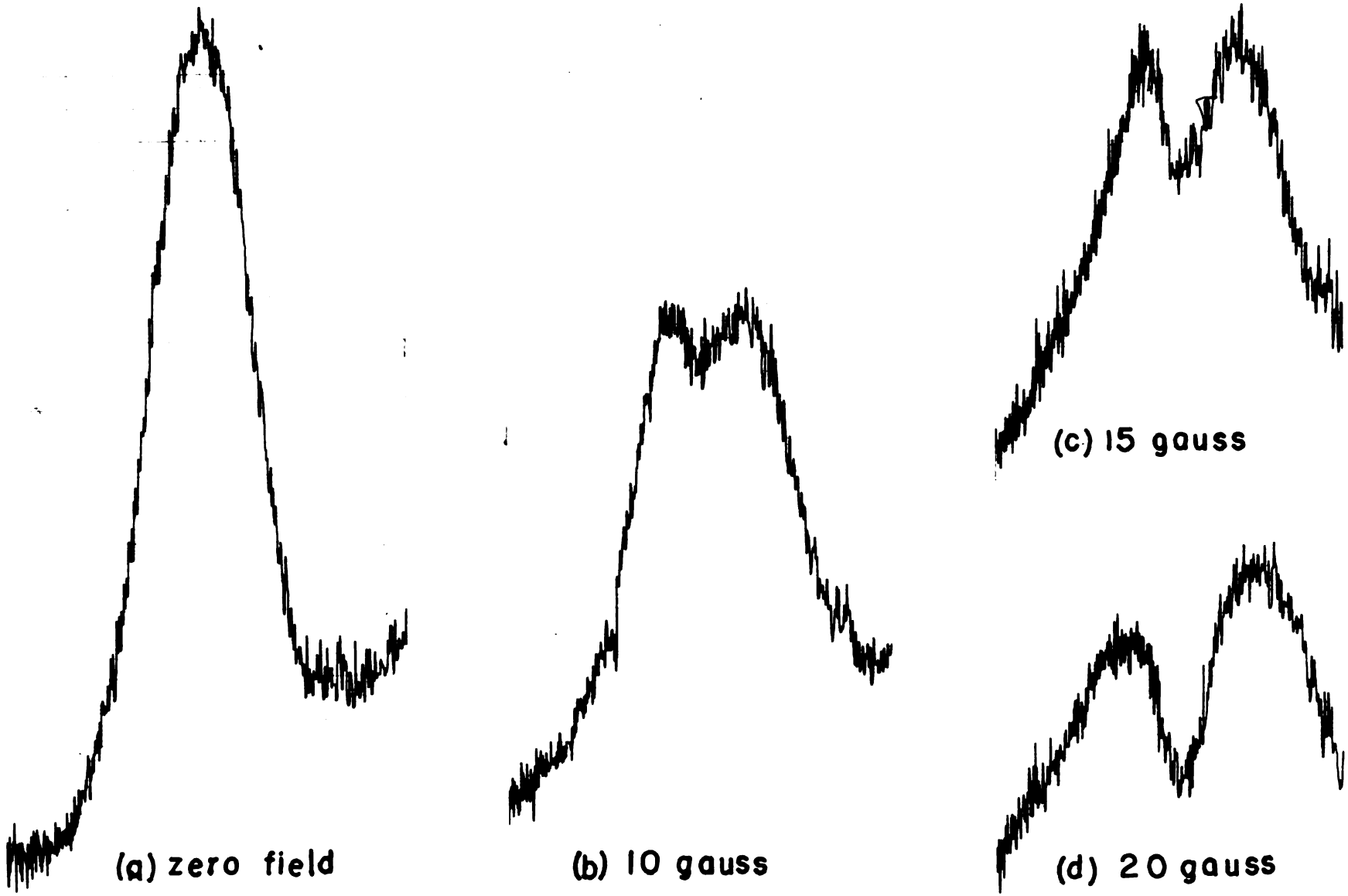

Fig. 10.--Splitting of a Single Line as a Function of Zeeman Field Intensity.

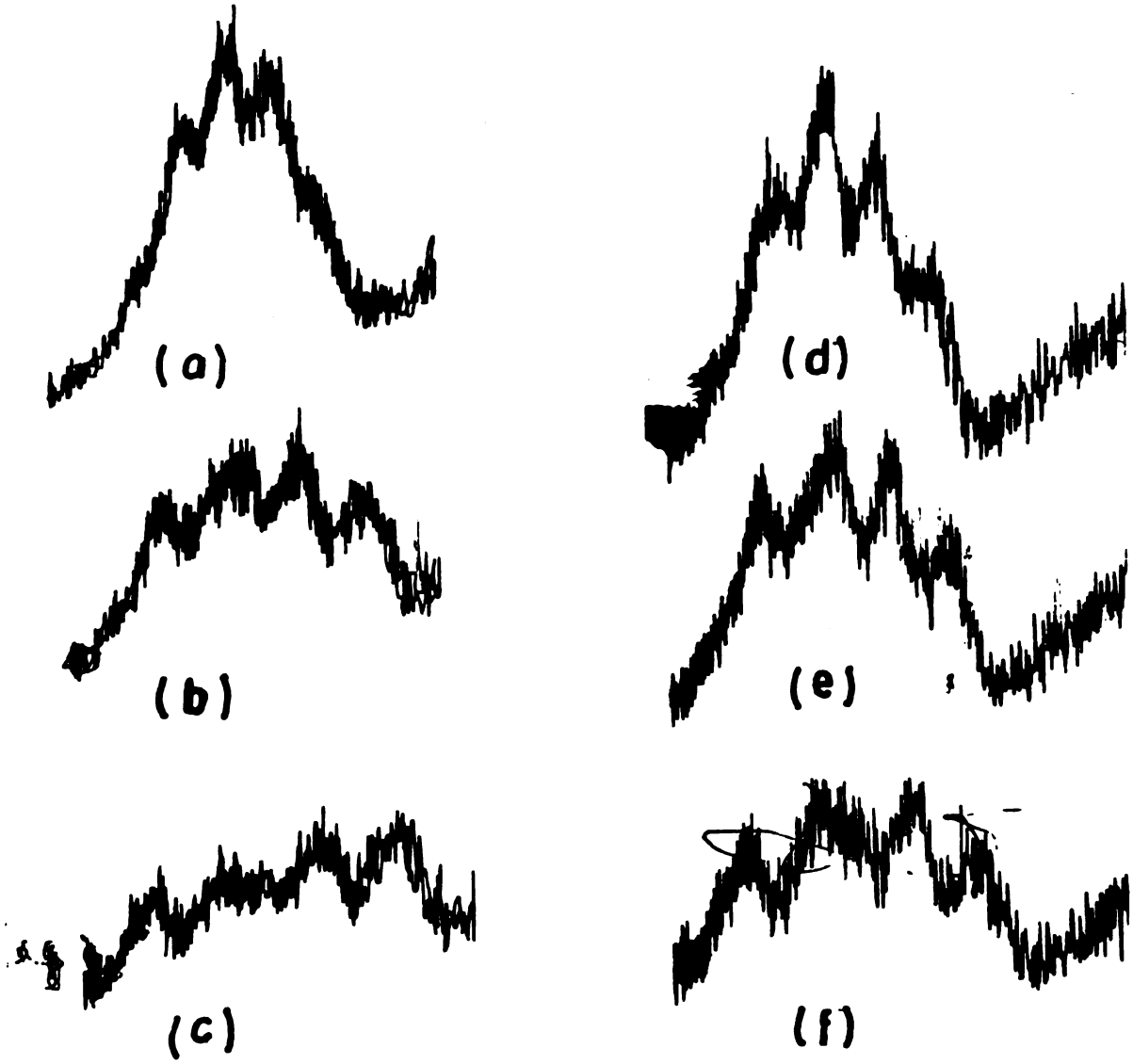

Fig. 11.--Splitting of Resonance Lines Resulting From Two or More Physically Inequivalent Nuclear Sites in the Unit Cell of the Crystal of Sodium Chlorate.

BIBLIOGRAPHY

1. J. H. Smith, E. M. Purcell, and N. F. Ramsey. Phys. Rev. 108, 120 (1957).

2. C. Dean. Phys. Rev. Vol. 96, No. 4, 1053-1059, Nov. 15, 1954.

3. T. P. Das and E. L. Hahn. Solid State Physics, Supplement 1, Nuclear Quadrupole Resonance Spectroscopy, pp. 5-12.

4. C. Dean and R. V. Pound. J. Chem. Physics 20, 195, 1952.

5. Duchesne and Monfils. Comptes Rendus 238, 1801, (1954).

6. Buyl, Boden and Dantreppe. Comp. Ren. 233, 1101 (1951)

7. Strukturburicht, Band 1. P. 154, 1913-1928.

8. Henry Cox and Dudley Williams. J. Chem. Phys. 30, 633 (1960).

9. P. J. Bray. J. Chem. Phys. 23, No. 4, 703-706 (1955).